Nuclear Materials and Energy 19 (2019) 335–339

Contents lists available at ScienceDirect

Nuclear Materials and Energy

journal homepage: www.elsevier.com/locate/nme

Initial results from the hotspot detection scheme for protection of plasma facing components in Wendelstein 7-X

A. Ali[*,a,c], H. Niemann[a], M. Jakubowski[a,h], T. Sunn Pedersen[a], R. Neu[b,c], Y. Corre[g], P. Drewelow[a], A. Puig Sitjes[a], G. Wurden[f], F. Pisano[e], B. Cannas[e], Y. Gao[d], M. Ślęczka[h], the W7-X Team[1]

[a] Max-Planck-Institut für Plasmaphysik, Wendelsteinstr. 1, Greifswald 17491, Germany
[b] Max-Planck-Institut für Plasmaphysik, Boltzmannstr. 2, Garching 85748, Germany
[c] TUM, Department of Mechanical Engineering, Boltzmannstra. 15, Garching 85748, Germany
[d] Forschungszentrum Jülich GmbH, Jülich 52425, Germany
[e] University of Cagliari, Cagliari 09124, Italy
[f] Los Alamos National Laboratory, Los Alamos 87545, USA
[g] CEA, IRFM, Saint-Paul-Lez-Durance F-13108, France
[h] University of Szczecin, Szczecin Poland

ARTICLE INFO

Keywords:
W7-X
Divertor
Plasma facing components
Heat load
Infrared
Surface layers
Tore supra

ABSTRACT

One of the main aims of Wendelstein 7-X (W7-X), an advanced stellarator, is to investigate the quasi-steady state operation of magnetic confinement devices for nuclear fusion, for which power exhaust is an important issue. A dominant fraction of the energy leaving from the confined plasma region will be removed by 10 so-called island divertor units, which are designed to sustain a maximum heat flux of up to 10 MWm^{-2}. An essential prerequisite for the safe operation of a steady-state device is automatic detection of hot spots and other abnormal events. Simple temperature limits in infrared (IR) thermographic images will not be enough on their own, because of plasma-generated surface coatings and other effects summarized in the following. To protect divertor elements from overheating, and to monitor power deposition onto the divertor elements, near real-time hotspot detection algorithms for the analysis of carbon plasma facing components (PFCs) were implemented and tested in the GLADIS facility.

One of the difficulties in hotspot detection in a carbon-based machine is the deposition of plasma impurities as layers with a reduced thermal connection to the underlying bulk material. We have developed and successfully tested a method to classify surface layers and benchmarked the performance of the method with the Tore Supra IR data operating with actively cooled carbon PFCs. The surface layers can be detected in a steady plasma discharge during the initial rise and decay in temperature when a strike line touches parts of the divertor or wall. It can also be detected by modulating electron cyclotron resonance heating (ECRH) input power. This feature allows detection of overheated areas while reducing false positives. For the recent operational campaign, inertially cooled test divertor units (TDU) were installed to prepare for steady-state operation with water-cooled divertor units. Automatic, near real-time detection of hot spots and identification of surface layers in the W7-X divertor are presented. Results are compared with a best fit estimate of the heat transmission coefficient α which is used to calculate heat flux onto the divertor in the presence of surface layers.

1. Introduction

W7-X is an optimized stellarator, designed to allow steady-state plasma discharges of up to 30 minutes in length. The PFCs which are subject to the most substantial power loads are 10 divertor units. The divertor of W7-X is subdivided into units which are composed of about 890 PFCs containing about 14,000 flat carbon fiber composite (CFC) NB31 tiles [1]. These CFC armor tiles are bonded via an Active Metal Casting copper (AMC-Cu) interlayer to a copper chromium zirconium (CuCrZr) cooling structure as shown in Fig. 1. The Cu interlayer (so-called bi-layer) is used to reduce stresses and strains in both the CFC area as well as the metallic section [2].

* Corresponding author to: Max Planck Institute for Plasma Physics, Wendelsteinstr. 1, 17491 Greifswald, Germany.
E-mail address: adnan.ali@ipp.mpg.de (A. Ali).
[1] Max-Planck-Institut für Plasmaphysik, Wendelsteinstr. 1, 17491 Greifswald, Germany

https://doi.org/10.1016/j.nme.2019.03.006
Received 1 August 2018; Received in revised form 4 March 2019; Accepted 5 March 2019

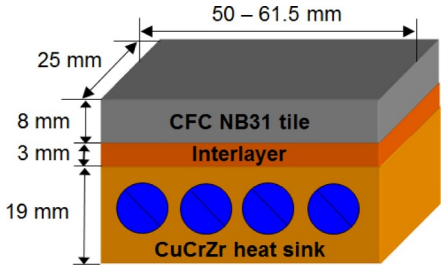

Fig. 1. Schematic design of a CFC tile. The gray surface on the top is composed of CFC NB31 type bulk surface connected to CuCrZr cooling structure with the help of Cu interlayer. Courtesy J.Boscary.

A possible overheating of PFCs may lead to defects at the bonding of the CFC tiles to the Active Metal Casting (AMC) interlayer [3]. The required timescales for detection and reaction to avoid any damage on PFCs is approximately 1 second. However, prior reactions will be taken e.g., by reducing the heating already at lower temperatures. The exact threshold will be defined in the future once the absolute error of the IR calibration is known. Thus, detection of such defects in near real-time is necessary during plasma operation to reduce the local heat flux if required. Such systems to prevent overheating of PFCs are also developed in other fusion devices, e.g., JET [4] and ASDEX Upgrade [5].

Each divertor module at W7-X consists of 250 mm to 500 mm long and 50 mm to 61.5 mm wide individual target elements. In the recent campaign of W7-X, inertially cooled carbon-based test divertor units (TDU) are installed. The TDU divertor surfaces have a shape that is nearly identical to that of the future water-cooled divertor.

2. W7-X hotspot detection scheme

Infrared Diagnostic at W7-X. A medium wavelength infrared (MWIR) camera with a spectral wavelength range of 3 μm to 5 μm is mounted inside a prototype endoscope [6,7]. The optical setup of the prototype endoscope makes it possible to cover the entire view of the divertor in one module as can be seen in Fig. 2. The integration time of the IR camera is varied from 50 μs to 200 μs depending on the expected surface temperature on the divertor. The camera operates typically at full frame rate of 106 Hz. The spatial resolution of the endoscope varies between 4 to 12 mm per pixel between the low iota (TM1-4h, TM1-3v) and high iota (TM7-9h) region (see Fig. 2). For further information about the IR diagnostic at W7-X, see [7]. Control software described in [8,9] with a dedicated acquisition workstation was used to control the camera and acquire results from the graphics processing unit (GPU).

Hotspots. The primary strategy of the W7-X IR imaging diagnostic is to detect hot spots on the carbon plasma facing components with thermal event recognition [8,9]. Excessive power loads onto the PFCs can damage the upper surface of the material which can lead to cracks in the structure. They can also appear because of delamination in the water-cooled tile [3,8] and need to be clearly distinguished from overheating due to surface layers to avoid false alarms. For this reason, hot spots need to be detected in near real-time to provide early response to the central control system of W7-X [3].

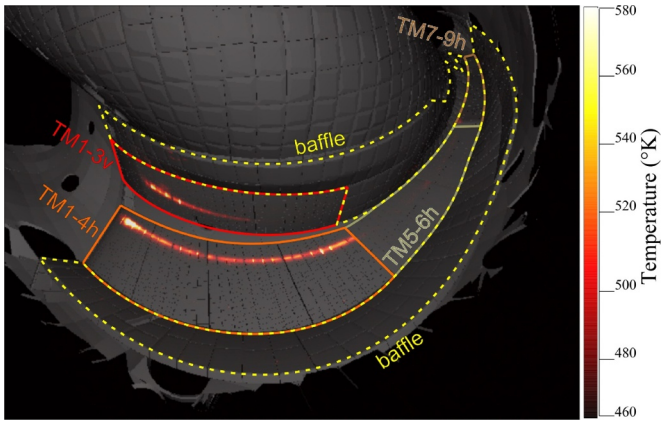

Fig. 2. Scene model showing lower divertor mapped to IR temperature data in Kelvin (K). It shows the horizontal divertor range from target module 1 to 9 (TM1-9h) and vertical divertor from 1 to 3 (TM1-3v).

Surface Layers. In general, the composition of the local distribution of impurity depositions like carbon, hydrogen, oxygen, boron or iron contribute to the build-up of surface layers. Due to weaker thermal connection to the bulk material, areas where impurities are re-deposited display a higher temperature and could be interpreted as hot spots. In many fusion related plasma confinement experiments, classification and detection of IR emission because of erosion and re-deposition during the interaction of plasma with the material are investigated in-depth [10]. Such investigation of plasma material interaction are necessary regarding safety diagnostics as it can lead to uncertainties in the thermographic monitoring and heat flux calculation as has already been observed on W7-AS [11,12]. Due to these complications, heat fluxes were partially overestimated up to a factor of 4 during the W7-AS operation [12]. The numerical methods presented in this work are able to detect hot spots in near real-time, as well as distinguish surface layers from hot spots due to e.g. melting of the PFCs. This feature reduces the chance of false alarms caused by very high temperatures on the net deposition regions [3,8].

Numerical Method. For simulating the behavior of surface layers on W7-X PFCs, FEM simulations were conducted, by overlaying a unconnected layer on top of the bulk surface [13]. The temperature evolution of PFCs with and without surface layers is shown in Fig. 3.

The apparent temperature on the area where surface layers are present increases much faster as compared to a clean surface whereas during the cooling phase, the energy is dissipated much faster in the form of radiation, which is why the surface layers cool down much faster as compared to a clean surface. A numerical method based on the normalized derivative of the temperature evolution of PFCs for detecting surface layers was developed that is defined in Eq. (1) as

$$\mathrm{norm}[t,\ T] = \frac{\partial_t T(t)}{T(t)}, \tag{1}$$

where T(t) is the surface temperature of a tile and $\partial_t T(t)$ is the partial derivative of temperature during the initial and decay phase. The $\mathrm{norm}_{[t,T]}$ of a surface layer will be higher during the initial rise time and lower during the initial decay time as compared to a clean surface that is without any deposition of layers. A user-defined threshold on $\mathrm{norm}_{[t,T]}$ is used to identify areas with surface layers during plasma operation. The algorithm is implemented using the CUDA library for graphics processing unit (GPU) computation. The usage of a GPU increases the performance of the numerical method for large datasets of thermographic images. Enhancement in the performance of the method

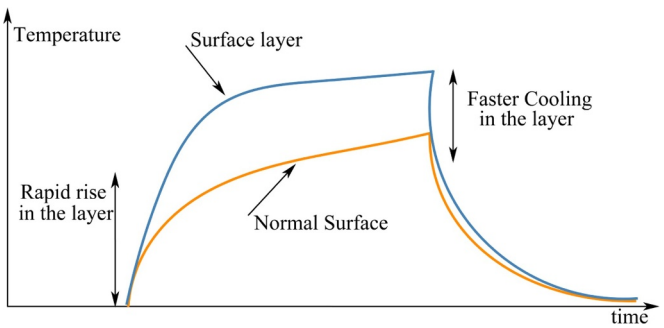

Fig. 3. Schematic of a temperature evolution of a PFC show with and without surface layers.

by a factor of 100 was achieved as compared to its initial state [3]. In previous publications, we have shown that the combination of a $\text{norm}_{[t,T]}$ criterion with a maximum allowed surface temperature T(t) can be used to distinguish between elevated temperatures that are due to surface layers and therefore unproblematic, and elevated temperatures due to overload, which are problematic [3,8].

Tore Supra Limiter. For bench-marking the numerical method to detect the areas where surface layers are present on water-cooled PFCs, thermographic data from Tore Supra (TS) looking at the Toroidal Pump Limiter (TPL) was analyzed. The TPL is made of 6 mm thick CFC tiles assembled on CuCrZr actively cooled body (thus based on the same technology as foreseen in the W7-X divertor modules). The TS-IR endoscopes were equipped with two IR cameras with spectral wavelength range of 3 μm to 5 μm. Three viewing lines, two for 2 sections of 35° of the TPL located at the bottom of the machine and one line looking at the heating antenna were used [14]. The spatial resolution on the TPL was between 7 mm to 10 mm in the center and outer part of the image respectively. For a standard TS plasma discharge (2MW injected power, 1 MA plasma current), healthy PFC located in net erosion area (with no surface layer) have maximum surface temperatures of around 350°C.

The part of the limiter with surface layers, located mainly at the periphery of the erosion areas, shows higher surface temperatures of more than 650°C which can be seen in Fig. 4. The $\text{norm}_{[t,T]}$ on the areas where surface layers are expected is higher as compared to a normal surface area which can be seen in Fig. 5. In the current case, the user-defined threshold of $\text{norm}_{[t,T]}$ for the areas with surface layers was set to a value of 7. The surface layers results from TS data can be seen in Fig. 6. The two ROIs used to extract the temperature evolution used in Figs. 4 and 5 are shown in Fig. 6 a. The areas are at an equal distance from the strike line, to demonstrate that the differences in T and $\text{norm}_{[t,T]}$ are not just due to the heat flux received.

The surface layer detected by the algorithm shows good agreement with visual inspection and previous IR data analysis [10,15]. These experimental results verified that the numerical method can be used to detect the surface layers inside a fusion device.

3. Comparison of methods used for detecting surface layers at W7-X.

To obtain the heat flux on the divertor targets, information about surface temperature, spatial calibration, and the material properties are necessary requirements. If these parameters are available, the heat flux can be calculated using the THEODOR (THermal Energy Onto DivertOR) code which solves the heat diffusion equation [16]. Further details regarding the heat flux calculation can be found in [5,16–18]. The most common practice for refining the heat flux calculation in the presence of surface layers is by estimating the heat transmission

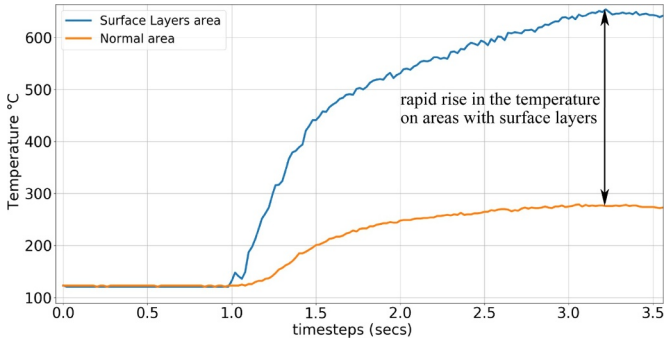

Fig. 4. Surface temperature evolution of two different areas on TPL as shown in Fig. 6 a. The blue curve shows the maximum temperature on the areas where surface layers are expected. The orange curve show the area where no surface layers are expected. (For interpretation of the references to colour in this figure legend, the reader is referred to the web version of this article.)

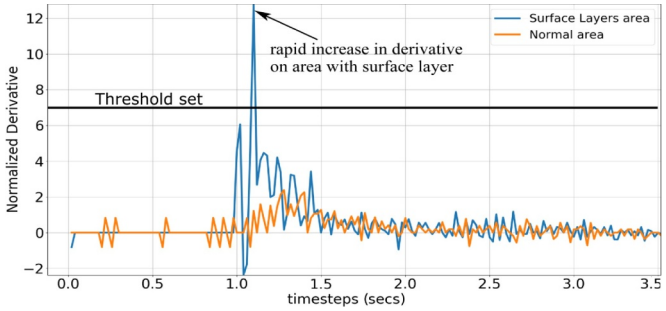

Fig. 5. $\text{norm}_{[t,T]}$ for areas where the surface layers are expected is shown in blue and normal surface in orange. (For interpretation of the references to colour in this figure legend, the reader is referred to the web version of this article.)

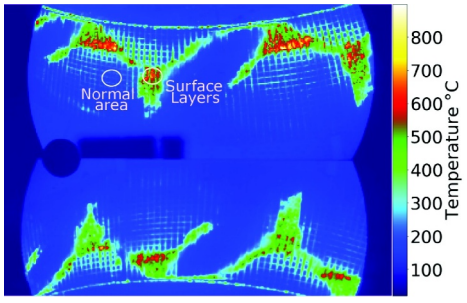

(a) Surface Temperature on the Tore Supra Limiter

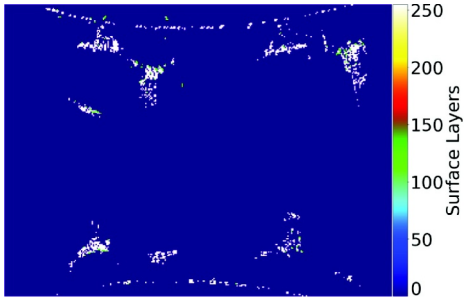

(b) Surface Layers detected by the $\text{norm}_{[t,\ T]}$ threshold method

Fig. 6. Results from Tore Supra showing surface temperature on the TPL taken from an IR camera. Fig. 6 b show a binary detected surface layers during rise (white) and (green) decay time. The results shown in Fig. 6 b are surface layers (in white color) detected during the rise time of the modulated pulse and are marked with a value of 255. (For interpretation of the references to colour in this figure legend, the reader is referred to the web version of this article.)

coefficient α in $\text{Wm}^{-2}\text{K}^{-1}$ which is defined in Eq. (2) as

$$\alpha = \frac{\lambda layer}{dlayer}, \tag{2}$$

where $\lambda layer$ is the heat conductivity of the layer and $dlayer$ is the thickness of the layer. Further details regarding the heat transmission coefficient α can be found in [19]. Small values of α reflect weakly coupled (small $\lambda layer$) or thick (large $dlayer$) surface layers. As the layer thickness and heat conductivity are unknown parameters, α is estimated iteratively. Too high values of α usually result in overestimated heat fluxes during the plasma discharge and negative heat fluxes at the end. The actual heat flux during an experiment is not known a priori, but the iterative procedure can be constrained sufficiently by the (physically obvious) requirement that the plasma heat flux is never negative and must be close to zero at the end of a plasma pulse. The iteration thus follows:

$$\alpha_{i+1}(s) = \alpha_i(s) b_i^{\epsilon(s)}, \tag{3}$$

where $b_i = 1 + b/\sqrt{i}$ reduces after each step. The free parameter b (here set to 0.5) controls the convergence speed and the resilience against numerical fluctuations. How strongly alpha (α) is adjusted in the next iteration depends on $\epsilon(s)$ as the ratio between the minimal (negative) heat flux at this point and absolute value of the most extreme minima along a profile. As a stop criteria for the iterations, it is assumed that the residual negative minima amount to less than 1% of the observed maximal heat flux. In the current state, the limit is set to 200 iterations.

$$\frac{|q_{\min-\text{low}}|}{\max(q_{\max-\text{high}}(s))} < 1\%. \tag{4}$$

The iterative method to find α is computationally expensive [19]. This feature prevents the code's usage in real-time applications and is the main reason for adapting a faster method of estimation of the layers. To compare the results obtained from the numerical method to detect surface layers as mentioned in Eq. (1), it was compared with the heat transmission coefficient α obtained from the heat flux calculation. The α values can be used to identify areas where surface layers affect the heat flux calculation.

The values of α obtained from the iterative method as mentioned in Eq. (3) are projected on the 2D model of a W7-X divertor module as seen in Fig. 7 b. The darker blue areas in Fig. 7 b show small values of α where surface layers are detected, whereas the orange area shows normal surface where no deposition was detected. The surface layer result obtained from the numerical method in Eq. (1) which is processed in GPU is projected on a simplified 2D model of the divertor as seen in Fig. 7 c. The control software [8,9] uses the numerical method and classifies the surface layers based on the state when they were detected.

The results of the two numerical methods for detecting the surface layers as shown in Fig. 7 b and c are overlayed to find the matching areas. This overlaying provides meaningful information to find the best threshold for $\text{norm}_{[t,T]}$, which matches well with the regions of lower α values. The histogram of α on the areas where the numerical method detected surface layers can be seen in Fig. 8.

The majority (90% to 99% in most cases) of α values lies below 5×10^5, which is used as a cut-off range for the region with surface layers. The results achieved from the analysis prove that the numerical method can be used alternatively to find areas that have low α values and by that indicates the presence of surface layers.

It is important to mention here that these results show the comparison of areas where the surface layers are detected by the numerical method which matches with the low α values in those locations but the inverse is not proven yet. There can be areas where the α correction method detected surface layers and the numerical method was not able to successfully detect them. However, this difference is still under analysis in order to find an optimal way to resolve this issue.

The numerical method depends on the relative background offset level (roughly 20 K above the background noise level) which may change during the day. Furthermore, in some cases the numerical method is unable to detect surface layers; this requires further analysis. This failure can be either due to lower heating of the divertor surface (temperature values lying below the offset level), low thickness of the surface layers or due to $\text{norm}_{[t,T]}$ values lower than the criterion parameters. Lower values of $\text{norm}_{[t,T]}$ may be due to rise in the background temperature during the day. However the influence of background temperature will reduce significantly in the future campaigns when water cooled PFCs will be installed.

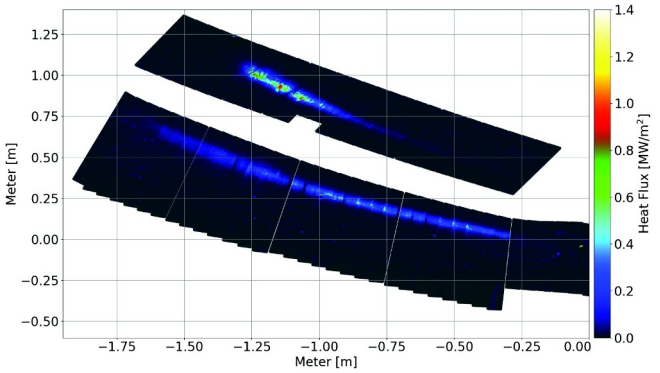

(a) Projection of the heat flux mapped on the horizontal and vertical divertor of W7-X. The maximum heat flux on the vertical divertor is more than 1 MW/m^2.

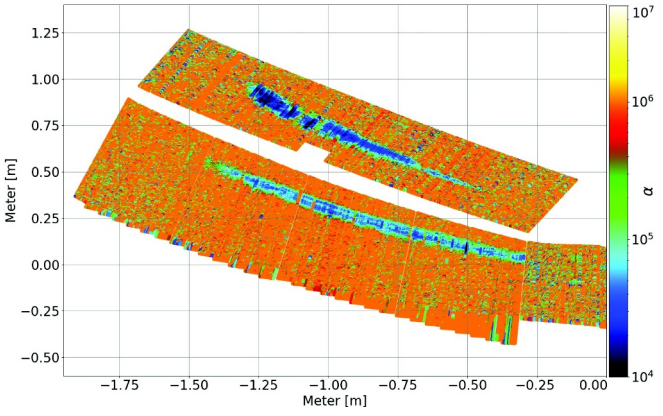

(b) Projection of heat transmission coefficient α on the horizontal and vertical divertor. The dark blue color shows lower values of α which correspond to the location of surface layers. The values of α below 5×10^5 are linked to surface layers.

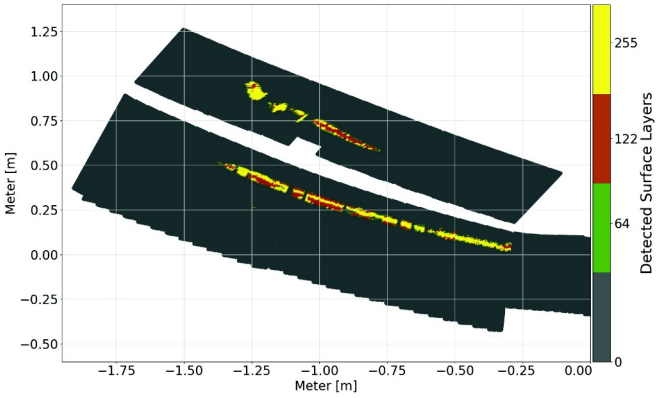

(c) Projection of surface layers detected on the W7-X horizontal and vertical divertor by the numerical method implemented in GPU. The yellow color labels the surface layers during rise-time detection. The green color labels surface layers during decay-time detection. The brown color labels surface layers in when both rise and decay-time detection.

Fig. 7. Comparison of α values from the heat flux calculation and the surface layer results from numerical algorithm mapped to a simplified 2D model of the W7-X divertor for shot number #20171101.012.

4. Outlook and summary

In this work, experimental performance of a near real-time system for detection of hot spots was evaluated. An automated method for identification of surface layers due to erosion and re-deposition of armor carbon tiles of the W7-X divertor was implemented. The numerical method shows promising results to detect surface layers on the carbon-based inertially cooled test divertor unit in W7-X. The results

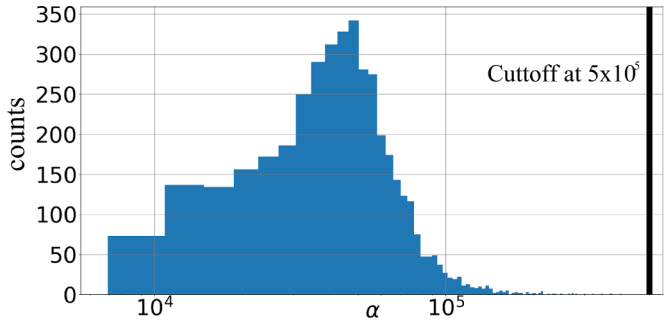

Fig. 8. Histogram showing the distribution of α values on the areas which matches with the surface layers detected by the numerical algorithm for shot number #20171101.012. The threshold for the minimum value of α for surface layers is set as 5×10^5.

from the numerical method computed by GPU were compared with the α values obtained from the heat flux calculation. The numerical method was successfully validated on water-cooled PFCs using the thermal images from Tore Supra. This approach robustly prevents false positives (unnecessary plasma terminations) due to surface layers in the studied situations, but it remains to be seen in long-pulse operation which other versions of false positives may unnecessarily terminate plasma operation.

Acknowledgments

This work has been carried out in Eurofusion Consortium and received funding from Euratom research and training programme 2014–2018 under grant agreement No 633053. The views and opinions expressed herein do not necessarily reflect those of the European Commission.

Supplementary material

Supplementary material associated with this article can be found, in the online version, at 10.1016/j.nme.2019.03.006

References

[1] G. Pintsuk, J. Compan, J. Linke, P. Majerus, A. Peacock, D. Pitzer, M. Rödig, Mechanical and thermo-physical characterization of the carbon fibre composite NB31, Phys. Scr. T T128 (2007) 66–71.
[2] H. Greuner, B. Böswirth, J. Boscary, P. Chaudhuri, J. Schlosser, T. Friedrich, A. Plankensteiner, R. Tivey, Cyclic heat load testing of improved CFC/cu bonding for the w 7-x divertor targets, J. Nucl. Mater. 386–388 (2009) 772–775.
[3] A. Rodatos, H. Greuner, M.W. Jakubowski, J. Boscary, G.A. Wurden, T.S. Pedersen, R. König, Detecting divertor damage during steady state operation of wendelstein 7-x from thermographic measurements, Rev. Sci. Instrum. 87 (2016) 1–8.
[4] G. Arnoux, S. Devaux, D. Alves, I. Balboa, C. Balorin, N. Balshaw, M. Beldishevski, P. Carvalho, M. Clever, S. Cramp, J.L. De Pablos, E. De La Cal, D. Falie, P. Garcia-Sanchez, R. Felton, V. Gervaise, A. Goodyear, A. Horton, S. Jachmich, A. Huber, M. Jouve, D. Kinna, U. Kruezi, A. Manzanares, V. Martin, P. McCullen, V. Moncada, K. Obrejan, K. Patel, P.J. Lomas, A. Neto, F. Rimini, C. Ruset, B. Schweer, G. Sergienko, B. Sieglin, A. Soleto, M. Stamp, A. Stephen, P.D. Thomas, D.F. Valcárcel, J. Williams, J. Wilson, K.D. Zastrow, A protection system for the JET ITER-like wall based on imaging diagnostics, Rev. Sci. Instrum. 83 (2012).
[5] B. Sieglin, M. Faitsch, A. Herrmann, S. Martinov, T. Eich, Real-time infrared thermography at ASDEX upgrade, Fusion Sci. Technol. 69 (2016) 580–585.
[6] M.W. Jakubowski, C. Biedermann, R. König, A. Lorenz, T. Sunn Pedersen, A. Rodatos, Development of infrared and visible endoscope as the safety diagnostic for steady- state operation of wendelstein 7-x, QIRT 100 (2014).
[7] M. Jakubowski, P. Drewelow, J. Fellinger, A. Puig Sitjes, G. Wurden, A. Ali, C. Biedermann, B. Cannas, D. Chauvin, M. Gamradt, H. Greve, Y. Gao, D. Hathiramani, R. König, A. Lorenz, V. Moncada, H. Niemann, T.T. Ngo, F. Pisano, T. Sunn Pedersen, Infrared imaging systems for wall protection in the w7-x stellarator (invited), Rev. Sci. Instrum. 89 (2018) 10E116.
[8] A. Ali, M. Jakubowski, H. Greuner, B. Böswirth, V. Moncada, A.P. Sitjes, R. Neu, T.S. Pedersen, W.-X. Team, Experimental results of near real-time protection system for plasma facing components in wendelstein 7-x at GLADIS, Phys. Scr. T170 (2017).
[9] A. Puig Sitjes, M. Jakubowski, A. Ali, P. Drewelow, V. Moncada, F. Pisano, T.T. Ngo, B. Cannas, J.M. Travere, G. Kocsis, T. Szepesi, T. Szabolics, W.-X. Team, Wendelstein 7-x near real-time image diagnostic system for plasma-facing components protection, Fusion Sci. Technol. 74 (2018) 116–124.
[10] Y. Corre, C. Brosset, E. Dufour, D. Guilhem, C. Lowry, R. Mitteau, P. Monier-Garbet, B. Pegourie, E. Tsitrone, S. Vallet, Visualisation of the deposited layer on the toroidal pumped limiter of tore supra using IR data during disruptions, 32nd EPS Conf. Control. Fusion Plasma Physics. Contrib. Paper. 29 (2005) 4–7.
[11] D. Hildebrandt, F. Gadelmeier, P. Grigull, K. McCormick, D. Naujoks, D. Sünder, Thermographic observation of the divertor target plates in the stellarators w7-AS and w7-x, J. Nucl. Mater. 313–316 (2003) 738–742.
[12] D. Hildebrandt, A. Dübner, H. Greuner, A. Wiltner, Thermal response to heat fluxes of the w7-AS divertor surface submitted to surface modification under high temperature treatment, J. Nucl. Mater. 390–391 (2009) 1118–1122.
[13] A. Rodatos, Algorithm Development for Safe Operation of the Wendelstein 7-X Divertor, Technische Universität München, 2017 Doctoral thesis. http://nbn-resolving.de/urn/resolver.pl?urn:nbn:de:bvb:91-diss-20170331-1328685-0-8
[14] D. Guilhem, J. Bondil, B. Bertrand, C. Desgranges, M. Lipa, P. Messina, M. Missirlian, C. Portafaix, R. Reichle, H. Roche, A. Saille, Tore-supra infrared thermography system, a real steady-state diagnostic, Fusion Eng. Des. 74 (2005) 879–883.
[15] M. Mitteau, J.C. Vallet, R. Reichle, C. Brosset, P. Chappius, J.J. Cordier, E. Delchambre, F. Escourbiac, A. Grosman, D. Guilhem, M. Lipa, T. Loarer, J. Schlosser, E. Tsitrone, Evolution of carbon tiles during repetitive long pulse operation in TORE SUPRA, Phys. Scr. T T111 (2004) 157–162.
[16] A. Herrmann, W. Junker, K. Günther, S. Bosch, M. Kaufmann, J. Neuhauser, G. Pautasso, T. Richter, R. Schneider, A.U. Team, Energy flux to the ASDEX upgrade divertor plates determined by thermography and calorimetry, Plasma Phys. Control. Fusion 37 (1995) 17–29.
[17] A. Hermann, . ASDEX Upgrade Team, Limitations for divertor heat flux calculations of fast events in tokamaks, 28th EPS Conf. Control. Fusion Plasma Physics. Contrib. Paper. (2001) 2109–2112.
[18] B. Sieglin, M. Faitsch, A. Herrmann, B. Brucker, T. Eich, L. Kammerloher, S. Martinov, Real time capable infrared thermography for ASDEX upgrade, Rev. Sci. Instrum. 86 (2015).
[19] P. Drewelow, Investigation of Divertor Heat Flux Pattern and Their Correlation to the Edge Magnetic Field of the Plasma Confinement experiment LHD, Technische Universität Berlin, Berlin, 2013 Doctoral thesis. https://depositonce.tu-berlin.de/handle/11303/4120 . doi:https://doi.org/10.14279/depositonce-3823